Journal of Electroceramics, 13, 627–636, 2004

Properties of $CaTi_{1-x}Fe_xO_{3-\delta}$ Ceramic Membranes

F.M. FIGUEIREDO,[1,2,*] M.R. SOARES,[3] V.V. KHARTON,[1,4] E.N. NAUMOVICH,[1,4] J.C. WAERENBORGH,[5] & J.R. FRADE[1]

[1] *Ceramics and Glass Eng. Department, CICECO, University of Aveiro, 3810-193 Aveiro, Portugal*
[2] *Science and Technology Dep., Universidade Aberta, R. Escola Politécnica 147, 1269-001 Lisbon, Portugal*
[3] *Lab. Central de Análises, University of Aveiro, 3810-193 Aveiro, Portugal*
[4] *Inst. of Physicochemical Problems, Belarus State University, 14 Leningradskaya Str., 220050 Minsk, Belarus*
[5] *Chemistry Department, Instituto Tecnológico e Nuclear, Estrada Nacional 10, 2686-953 Sacavém, Portugal.*

Submitted March 2, 2003; Revised February 2, 2004; Accepted March 19, 2004

Abstract. $CaCO_3$, TiO_2 and Fe_2O_3 were mixed in the appropriate stoichiometric quantities and calcined at 1100°C for 10 h. These powder mixtures were uniaxially pressed and sintered at temperatures ranging from 1350 to 1500°C for 2 h in order to obtain dense disk-shaped samples with nominal $CaTi_{1-x}Fe_xO_{3-\delta}$ ($x = 0.05$, 0.15, 0.20, 0.40 and 0.60) compositions. Dilatometry and *in situ* high temperature powder X-ray diffraction analysis showed a good agreement on the thermal expansion behaviour of these materials between room temperature and 1000°C. The estimated linear thermal expansion coefficient is close to 13×10^{-6} K^{-1} and is little affected by composition. No evidence for surface carbonation was detected in the infrared spectra collected on samples previously annealed in CO_2 atmospheres. The oxygen permeability measured at temperatures ranging from 750 to 1000°C goes through a sharp maximum for $x = 0.20$. This result is interpreted by structural differences related to change from disordered to ordered oxygen vacancies. The overall performance of $CaTi_{0.80}Fe_{0.20}O_{3-\delta}$ is compared to other mixed conducting materials.

Keywords: Calcium titanate, stability, thermal expansion, oxygen permeability

1. Introduction

Dense ceramic membranes formed from oxygen-ion and electron mixed-conducting materials are of considerable interest for use in the high temperature electrochemical separation of oxygen from gaseous mixtures as well as the use of the oxygen formed therefrom for the production of added value products (e.g. syn-gas) resulting from the partial oxidation of light hydrocarbon mixtures (e.g. natural gas) [1, 2]. The membrane material meets a certain number of requirements in order to provide stable performance under determined operation conditions. Apart from high values of ionic and electronic conductivities enabling competitive oxygen permeation fluxes, the membrane material should have high thermal stability and suitable coefficient of thermal expansion between ambient and operating temperatures. Chemical stability under significantly large oxygen activity gradients and in CO_2 (and CO) containing atmospheres is also a must. However, these are not sufficient. In order to maximise the oxygen flux, thin membranes (less than 0.5 μm) are used. In this case the kinetics of oxygen exchange at the membrane surfaces is often the main limiting factor to the measured flux [3]. Multilayered designs consisting of a dense mixed conducting oxide layer with a porous support of a similar material were proposed and tested with relative success [4, 5]. The porous layer provides the mechanical support whereas it can enhance the oxygen exchange reaction rate by increasing the surface area. Further improvements are achieved by depositing a catalytically active substance onto the porous layer. It is clear that the structural stability of the multilayered membranes during fabrication and operation is critically dependent on the

*To whom all correspondence should be addressed. E-mail: framos@cv.ua.pt

thermo-chemical compatibility of the respective membrane layers.

Multicomponent perovskite oxides are amongst the most promising materials for these applications. Those belonging to the $La_{1-x}Sr_xCo_{1-y}Fe_yO_{3-\delta}$ system were amongst the first to be disclosed [6]. Unfortunately, the Co-containing materials are chemically unstable and suffer excessive thermal expansion. Calcium titanate-based compositions may be of interest if Ti^{4+} is partially substituted by a lower valent transition metal cation. In particular, Fe^{3+} acts as an acceptor enhancing the oxygen ion vacancy ($V_O^{\bullet\bullet}$) concentration according to

$$2CaO + Fe_2O_3 \rightarrow 2Ca_{Ca}^{\times} + 2Fe_{Ti}' + 5O_O^{\times} + V_O^{\bullet\bullet} \quad (1)$$

and should also enhance the concentration of holes [1, 7]. Thus, both ionic and electronic conductivities were expected to increase, at least under oxidising conditions, when the contribution of electron holes exceeds the concentration of electrons. Actually, the effect of iron on the transport properties is far more complex, as revealed by the dependence of ionic conductivity on Fe content [7–12]. Structural changes explain the decrease in ionic conductivity for Fe contents above about 25%, by stabilising tetra-coordinated trivalent iron [11–16].

In this work, several properties of $CaTi_{1-x}Fe_xO_{3-\delta}$ are presented and reviewed in a systematic manner in view of the practical application of this family of materials for high temperature oxygen separation membranes. $Ca(Ti,Fe)O_{3-\delta}$ materials are stable [17], their thermal expansion coefficient (TEC) is moderate [18] and they certainly are cost-competitive.

2. Experimental

Nominal $CaTi_{1-x}Fe_xO_{3-\delta}$ ($x = 0.05$, 0.20, 0.40 and 0.60) materials were obtained by solid state reaction of high purity La_2O_3 (Merck), $CaCO_3$ (Merck) and Fe_2O_3 (Riedel-de-Haën). The reactants were wet-mixed in Nylon containers with zirconia balls during 2 hours, dried in a stove at 60°C, and calcined at 1100°C for 10 hours with heating/cooling rates of 4 K/min. The resulting powder was wet-milled, again dried, sieved through a 30 μm mesh and uniaxially pressed at 200 MPa into 1 mm thick disks with a diameter of 20 mm. Sintering was carried out in air at temperatures ranging from 1320 to 1500°C, increasing with decreasing Fe content, during 2 hours with heating/cooling rates of 5 K/min. The density of the ceramics, estimated from weight and geometry, was, for all samples, above 90% of the theoretical value obtained by X-ray diffraction. The good densification levels were confirmed by scanning electron microscopy (SEM) using a field emission gun Hitachi 4100S microscope equipped with a Rontec energy dispersive spectroscopy (EDS) detector. Sintering conditions and densities for the prepared ceramics are given in Table 1 while typical SEM micrographs of fractured ceramics are shown in Fig. 1.

Table 1. Sintering conditions and density of $CaTi_{1-x}Fe_xO_{3-\delta}$ ceramics.

x	Sintering temperature (°C)	Densification* (%)
0.05	1500	99
0.15	1410	91
0.20	1370	97
0.40	1320	96
0.60	1300	97

*% of theoretical. Average of 2 to 4 samples.

Room temperature and high temperature *in-situ* powder X-ray diffraction (XRD) patterns were obtained in a Phillips diffractometer using $Cu_{K\alpha}$ radiation with a scan speed of 0.1°/min and step width, 0.02°. The lattice parameters, estimated with a simple Pauling refinement of the XRD patterns using FullProof, were used to determine an apparent volume thermal expansion coefficient (VTEC). Values of linear thermal expansion coefficient (LTEC) were obtained from dilatometric measurements carried out in air from room temperature up to 1000°C with a constant heating rate of 5 K/min.

The formation of products of reaction $CaTi_{1-x}Fe_xO_{3-\delta}$ with CO_2 was assessed after keeping the powdered material in CO_2 atmosphere at room temperature for 25–27 hours. The infrared absorption spectra were recorded at room temperature on a Spectrum-1000 Fourier transform infrared (FT-IR) instrument (Perkin-Elmer). The spectra were collected in the range of 300–1200 cm^{-1} using the usual KBr pellet technique.

Total conductivity values were obtained by impedance spectroscopy (impedance analyser model 4284A LCR, Hewlett Packard) at temperatures ranging from 1000°C down to room temperature. The spectra were collected in the frequency range 20 Hz to 1 MHz using a 50 mV alternate signal. Further details of the spectra analysis are given elsewhere [19].

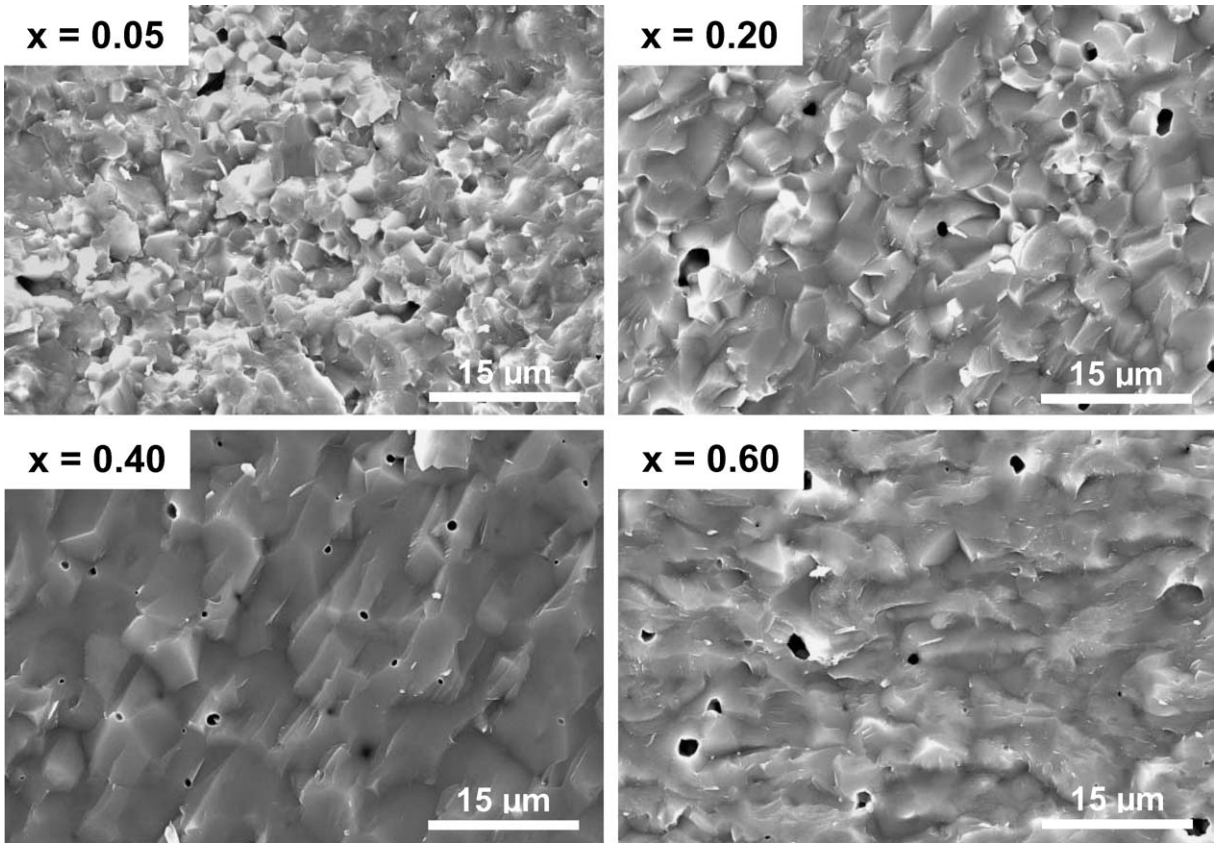

Fig. 1. SEM micrographs of $CaTi_{1-x}Fe_xO_{3-\delta}$ ceramics.

The oxygen permeability was measured at temperatures ranging from 750 to 1000°C under an oxygen partial pressure (Po_2) gradient established between atmospheric air and a variable value down to ca. 0.1 kPa. The measurements were carried out in a system consisting of a tubular zirconia oxygen electrochemical pump covered on the sides by a zirconia disk and the ceramic membrane under study, which are sealed to the pump with an appropriate glass to ensure gas tightness. The zirconia tube is used to electrochemically pump oxygen out of the chamber while the zirconia disk functions as an oxygen sensor to monitor the Po_2 variations inside the chamber (P_2), while that in the outside (P_1) is fixed by atmospheric air (21 kPa). The molecular oxygen permeation flux is obtained through

$$jo_2 = I_{pump}/(4FS) \quad (2)$$

where S is the surface area available for transport and F is the Faraday constant. All ceramic samples were verified to be free of percolated porosity by forcing a flow of compressed air (≈250 kPa) through the membrane under water and checking that no bubbles form on the permeate side. The existence of leaks through the sealings was assessed at the measuring temperatures by analysis of the transient recovery of P_2 to a value close to P_1, as described in ref. [20]. Further details and descriptions of the oxygen permeation measurements may be found elsewhere [18, 20, 21].

3. Results and Discussion

3.1. Structural Considerations

$CaTiO_3$ is the chemical formula of the mineral perovskite. Its structure has been widely studied. It has the classical cubic perovskite structure, at sufficient high temperatures, which can be indexed onto the Pm3m space group. However, at low temperature the oxygen

octahedra undergo a slight distortion causing a loss of symmetry; the room temperature XRD spectrum is easily indexed onto Pnma or Pbnm orthorhombic primitive cells [22]. The partial substitution of Ti^{4+} by Fe^{3+} in $CaTi_{1-x}FeO_{3-\delta}$ leads to the formation of oxygen vacancies to keep electroneutrality. The vacancies created upon moderate substitution levels (<20–30%), should be accommodated without great changes. At least for relatively high temperatures when thermal vibration is high enough, the oxygen vacancies are randomly distributed or only partially ordered in linear chains [12, 15]. This is the case for $CaTi_{0.95}Fe_{0.05}O_3$ which preserves the orthorhombic structure of the original perovskite at low temperature (Fig. 2(A)). At high temperature, an increase in symmetry is apparent from the *in situ* high temperature powder XRD spectra shown in Fig. 2(A); the diffraction peaks corresponding to the orthorhombic distortion tend to disappear as temperature increases while the main peaks become thinner.

When the oxygen vacancy concentration is over a certain value, approximately corresponding to $x = 0.5$, the chain growth yields long-range ordering and eventual formation of fully ordered phases. These phases have been studied for totally reduced materials (without any Fe^{4+}) and are relatively well known since the work from Grenier et al. [13, 14]. According to the model proposed by these authors, the vacancies are ordered into planes containing tetrahedral Fe^{3+} which alternate with planes containing octahedrally coordinated Ti^{4+} and Fe^{3+}. These sequences of tetrahedral (T) and octahedral (O) layers are formed in the (0k0) planes of the original $CaTiO_3$ cell (space group Pnma). The T:O ratio increases with increasing iron content and some stable structural motives, that correspond to OT, OOT and OOOT ordered sequences, are found for specific compositions: $Ca_2Fe_2O_5$ ($x = 1.00$), $Ca_3TiFe_2O_8$ ($x = 0.67$) and $Ca_4Ti_2Fe_2O_{11}$ ($x = 0.50$). All these phases have orthorhombic symmetry. In practice, deviations from these exact stoichiometries result in intergrowths of the more stable motives leading to the development of microdomains. Moreover, the presence of some Fe^{4+} in the structure may induce significant changes in the microdomain texture. For instance, the powder XRD spectra of partially oxidised $CaTi_{0.4}Fe_{0.6}O_{3-\delta}$ suggest cubic symmetry (space group Pm3m) from room temperature up to 900°C (Fig. 2B), while the totally reduced counterpart is clearly orthorhombic [12, 13]. Transmission electron microscopy (TEM) studies [23] were necessary to unveil the real structure of this material. The

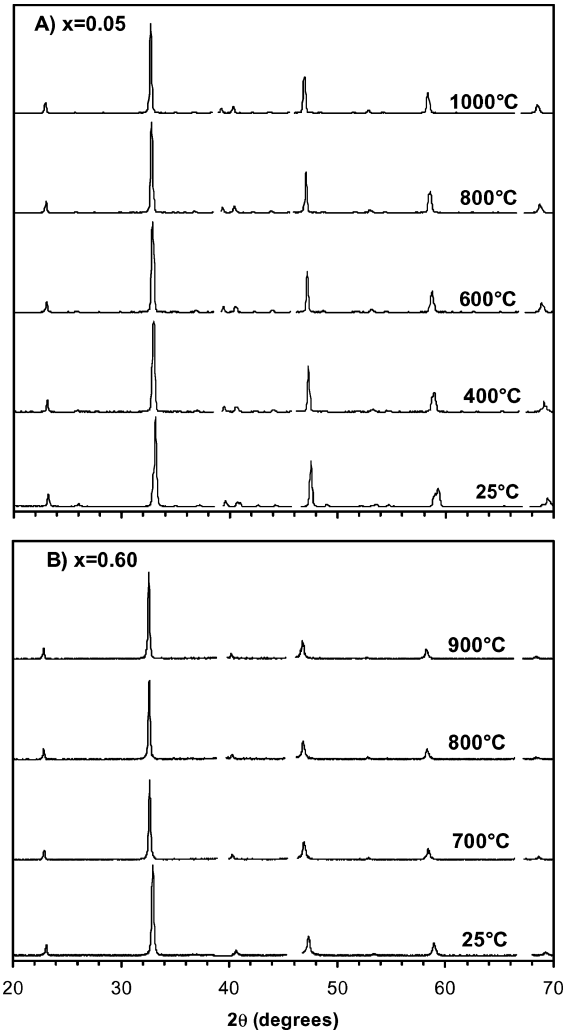

Fig. 2. In situ high temperature $CaTi_{1-x}Fe_xO_{3-\delta}$ powder XRD patterns: (A) $x = 0.05$; (B) $x = 0.60$. The gaps are due to the removal of the platinum peaks.

apparent pseudocubic symmetry evidenced by XRD actually corresponds to the symmetry of very small microdomains (<10 nm) aligned along three perpendicular directions in a manner that, metrically, each set of domains has cubic symmetry; $Ca_3TiFe_2O_8$ being the majority phase [23].

3.2. *Thermal Expansion*

The necessity of maintenance operations implies thermal cycling of the cells. Therefore, the TEC of the

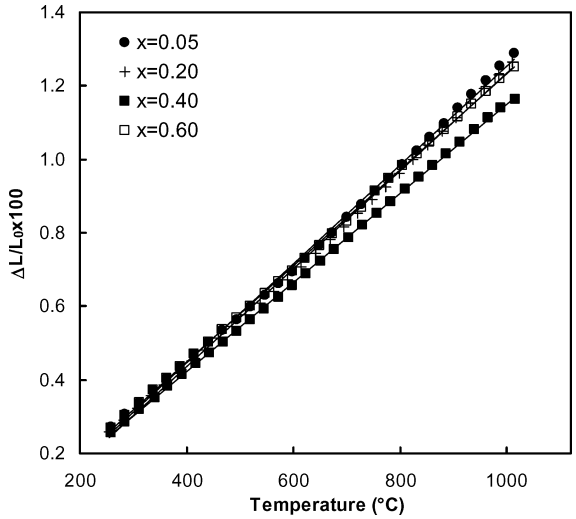

Fig. 3. Thermal expansion of $CaTi_{1-x}Fe_xO_{3-\delta}$ ceramics.

membrane material should be as low as possible, and constant in broad temperature ranges. Note that stresses resulting from thermal shock or thermal expansion mismatch with other cell components may be aggravated by chemical expansion under large Po_2 ranges. Also, the fabrication will be easier if the thermal expansion coefficient of the material is low [5]. As shown in Fig. 3, $CaTi_{1-x}Fe_xO_{3-\delta}$ ceramics are good candidates from this point of view. Firstly the relative elongation in the range 25–1000°C shows an almost linear dependence with temperature; secondly, the TEC values are moderate (12.3 to $13.4 \times 10^{-6}\,K^{-1}$); and finally, no significant effect of composition is apparent.

The characterisation of the thermal expansion behaviour of $CaTi_{1-x}Fe_xO_{3-\delta}$ ceramics was complemented with the analysis of the lattice volume variation by *in situ* high temperature powder XRD. Results in Table 2 show that, as expected, the lattice parameters increase with increasing temperature. Figure 4 furthermore shows that a linear positive correlation between the lattice volume and temperature is retained up to 1000°C and that hence the determination of the volume thermal expansion coefficient (VTEC) is possible from this set of data. The VTEC of a material may be approximated to the linear thermal expansion coefficient (LTEC) by the simple and well known relation LTEC = VTEC/3. The agreement between the thermal expansion coefficient (TEC) values obtained by dilatometry and XRD is, within expected errors, fairly good, as shown by Fig. 5.

Table 2.

Composition	Temp. (°C)	Space group	Lattice parameters		
			a(Å)	b(Å)	c(Å)
$x = 0.05$	25	Pnma	5.3822	5.4372	7.6416
	400	Pnma	5.4245	5.4460	7.6984
	600	Pnma	5.4422	5.4638	7.7242
	800	Pnma	5.4667	5.4653	7.7220
	1000	Pnma	5.4753	5.4775	7.7339
$x = 0.20$	25	Pnma	5.3876	5.4287	7.6417
	800	Pnma	5.4715	5.4727	7.7211
	900	Pnma	5.4769	5.4774	7.7330
	1000	Pnma	5.4831	5.4898	7.7427
$x = 0.40$	25	Pnma	5.4304	7.6455	5.3903
	400	Pnma	5.4457	7.6890	5.4430
	600	Pnma	5.4613	7.7005	5.4568
	800	Pnma	5.4736	7.7327	5.4724
$x = 0.60$	25	Pm3m	3.8246		
	400	Pm3m	3.8335		
	700	Pm3m	3.8505		
	800	Pm3m	3.8526		
	900	Pm3m	3.8595		

Numerous other perovskites with good electrical and electrochemical properties such as $Sr(Ti,Fe)O_{3-\delta}$ [24] $(La,Sr)(Co,Fe)O_{3-\delta}$ [6], $(La,Sr)(Ga,Fe)O_{3-\delta}$ [25] have higher TEC values and, perhaps more harmful

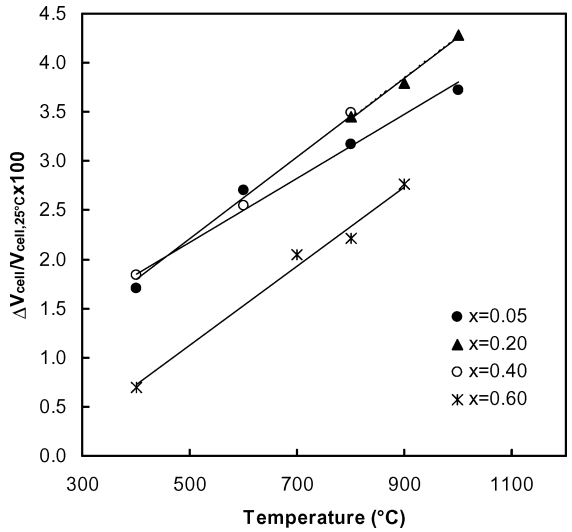

Fig. 4. Thermal expansion of the relative unit cell volume.

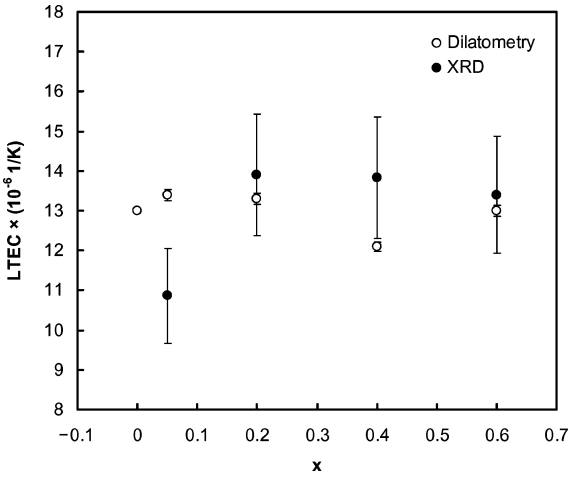

Fig. 5. Comparison of thermal expansion coefficients determined from dilatometry and high temperature *in situ* powder XRD data. The value for $x = 0$ was taken from ref. [36].

for practical proposes, these TEC values tend to increase sharply above a certain temperature. Such behaviour was associated to extensive oxygen losses, that cause lattice expansion [26] and hence higher TEC values, due to the change of the oxidation state of the transition metal cations. These changes are limited in $CaTi_{1-x}Fe_xO_{3-\delta}$, since the fraction of Fe^{4+}, as determined by Mössbauer spectroscopy, was never higher than 20% of the total number of Fe cations [15]. Moreover, detailed structural studies have shown that the reduction of Fe^{4+} leads mainly to the formation of tetrahedral Fe^{3+} and thus to ordered oxygen vacancies. The stabilization of iron oxidation states in $Ca(Ti,Fe)O_{3-\delta}$ over a broad range of temperature and Po_2 conditions leads us to predict a significant thermo-mechanical stability in typical operation and maintenance conditions of the membrane devices.

3.3. *Stability in CO_2 Atmospheres*

The reaction

$$SrTiO_3 + CO_2 \rightarrow SrCO_3 + TiO_2 \qquad (3)$$

has an estimated negative variation of Gibbs free energy of $\Delta G = -11.1$ kcal mol^{-1} ($T = 298$ K, CO_2 fugacity of 10^5 Pa), according to estimations based on thermodynamic data taken from ref. [27]. Indeed, a previous work has shown that $Sr_{0.97}Ti_{1-x-y}Fe_xMg_yO_{3-\delta}$ compounds react with CO_2 at room temperature forming $SrCO_3$ [28]. However, the formation of carbonaceous species at the surface may be enough to cause significant degradation of the membrane performance by hindering the exchange reactions. Moreover, the subsequent decomposition of strontium carbonate at higher temperature might compromise the mechanical integrity of the ceramics, especially for multilayered membranes. One used thermodynamic data [27] to predict the temperature ($T \approx 566$ K) at which reaction 3 should be reverted. The formation of $SrCO_3$ was also confirmed for other perovskite mixed conductors containing significant fractions of Sr (e.g. $La_{0.7}Sr_{0.3}Ga_{1-x}Fe_xO_{3-\delta}$ [25]).

As for $SrTiO_3$, the formation of $CaCO_3$ at room temperature according to:

$$CaTiO_3 + CO_2 \rightarrow CaCO_3 + TiO_2 \qquad (4)$$

is thermodynamically favourable ($\Delta G = -11.4$ kcal mol^{-1}, $T = 298$ K, CO_2 fugacity of 10^5 Pa). Thus, $CaTi_{1-x}Fe_xO_{3-\delta}$ should also be prone to react with CO or CO_2 forming calcium carbonate. One also used thermodynamic data [27] to predict the temperature range required to revert reaction 4 ($T > 621$ K). However IR analysis of powders of $CaTi_{1-x}Fe_xO_{3-\delta g}$ ept in a CO_2 atmosphere at room temperature did not reveal the presence of $CaCO_3$ (Fig. 6). The most intense absorption band expected for $CaCO_3$ ($\nu \approx 875$ s^{-1}) is absent in all spectra. Carbonation of $CaTi_{1-x}Fe_xO_{3-\delta}$ seems thus not to be of significance and improved chemical stability coupled with the thermo-mechanical stability is expected for this material in comparison to other Sr-containing compositions. Thus, it seems that the formation of carbonate by reaction of calcium titanate with CO_2 is sluggish, and that differences between the reactivity of calcium and strontium titanates at room temperature might be controlled by kinetics rather than thermodynamics.

In addition, one should take into account that titanates often accommodate significant fractions of A-site deficiency, which affects the activity of the earth alkaline species, and thus its reactivity with CO_2. Titanates might thus accommodate significant A-site deficiency without precipitation of titania, and formation of carbonates might be described as:

$$ATiO_3 + \Delta CO_2 \rightarrow \Delta ACO_3 + A_{1-\Delta}TiO_{3-\delta} \qquad (5)$$

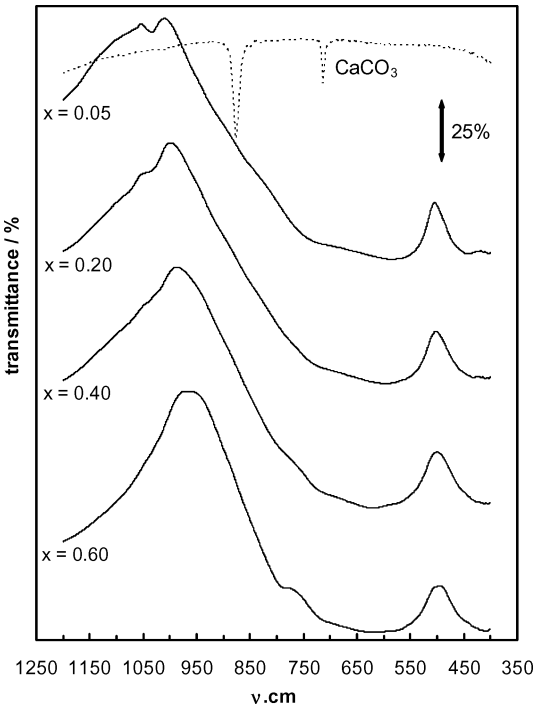

Fig. 6. Infrared spectra of $CaTi_{1-x}Fe_xO_{3-d}$ materials obtained at room temperature after exposure to CO_2. The spectrum of $CaCO_3$ is shown dashed for comparison.

where A = Ca, Sr. In this case, thermodynamic calculations based on reactions 3 or 4 are probably insufficient to predict the reactivity of these titanates with CO_2.

Although interpretation of the IR data is not a central object of the present work, a few simple remarks are presented. The spectrum of $CaTi_{0.95}Fe_{0.05}O_{3-\delta}$ is very similar to that of $CaTiO_3$ [29]. The minima at $\nu \approx 580$ and $\nu \approx 440\ s^{-1}$ were ascribed to the stretching of the TiO_6 octahedra, while bending of the Ti—O—Ti bonds and lattice vibrations modes should be observed for $\nu < 400\ cm^{-1}$. It can be seen that increasing the iron content leads to slight shifts of both these bands: towards higher frequencies for the $\nu \approx 580\ cm^{-1}$ band, and to lower values the $\nu \approx 440\ s^{-1}$. It is reasonable to associate these frequencies to the structural elements common to all materials (TiO_6 octahedra). On the other hand, the additional minimum observed for $CaTi_{0.4}Fe_{0.6}O_{3-\delta}$ ($\nu \approx 790\ cm^{-1}$) should be explained by the significant fraction of FeO_4 tetrahedra in the Fe-rich $CaTi_{1-x}Fe_xO_{3-\delta}$ compositions.

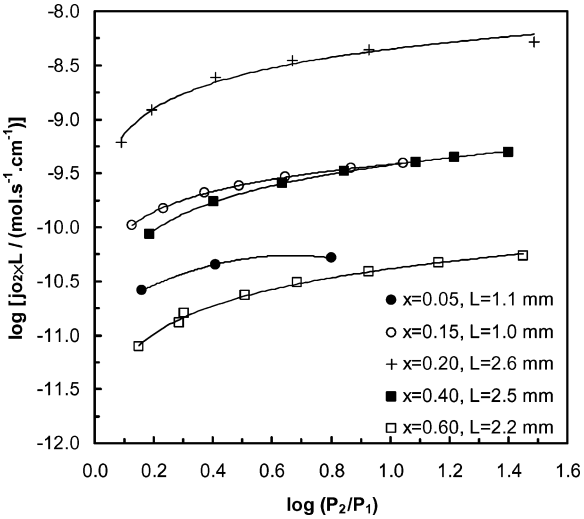

Fig. 7. Oxygen permeability of $CaTi_{1-x}Fe_xO_{3-\delta}$ as a function of the Po_2 gradient at 900°C.

3.4. *Oxygen Permeability*

Figure 7 shows the molecular oxygen flux, jo_2, normalised to the sample thickness, L, measured for different $CaTi_{1-x}Fe_xO_{3-\delta}$ ceramics. It can be seen that jo_2 increases about two orders of magnitude when x increases from 0.05 to 0.20. A marked decrease is observed for higher Fe-substitution levels. Fig. 8 further

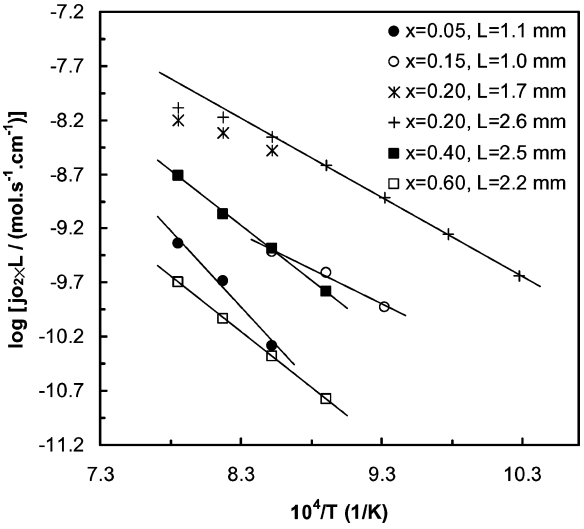

Fig. 8. Temperature dependence of the normalised oxygen permeability of $CaTi_{1-x}Fe_xO_{3-\delta}$ membranes at constant Po_2 gradient (log $(P_2/P_1) \approx 1$ and $P_1 = 21$ kPa).

shows that the trend apparent in Fig. 7 is extended over a relatively large temperature range from 700 to 1000°C. The values for the $x = 0.20$ are in good agreement with the literature [1] while no results are known for the remaining compositions.

The oxygen permeation depends on essentially three parameters, the ionic conductivity (σ_{ion}), the electronic conductivity (σ_{ele}) and the rate at which oxygen is exchanged at the surface of the material, expressed by an exchange coefficient (K). σ_{ion} and σ_{ele} may be combined in one ambipolar transport parameter (σ_{amb}) according to $\sigma_{amb} = \sigma_{ion}\sigma_{ele}/(\sigma_{ion} + \sigma_{ele})$. The oxygen permeation flux is then expressed as a function of the ambipolar transport coefficient as:

$$j_{O_2} = \frac{RT}{16F^2L}\int_{P_1}^{P_2} \sigma_{amb} d \ln Po_2 \qquad (6)$$

where F is the Faraday constant, R is the gas constant and T the absolute temperature. Equation (6) shows that the product $jo_2 \times L$ is independent of the membrane thickness if K is sufficiently high. On the contrary, slow oxygen surface exchange kinetics yields $jo_2 \times L$ values increasing with increasing L. The data in Fig. 8 suggest that jo_2 is partly limited by the surface exchange; at least for the composition with the highest jo_2. However, such a strong compositional effect is likely to be determined by the bulk properties. Under this assumption and since calcium titanate is predominantly a p-type electronic in the actual working conditions ($Po_2 > \approx 1$ Pa, $T > 700$°C) [7], the jo_2 values are limited by σ_{ion} (Eq. (6)). Indeed, the effect of composition on jo_2 is in excellent agreement with previously reported maximum in ionic conductivity of $CaTi_{1-x}Fe_xO_{3-\delta}$ for about 20 to 30 mol% of iron [1, 11, 17]. This maximum is consequence of the balance between a moderate oxygen vacancy concentration and a relatively disordered structure. Increasing x up to 0.20 creates a significant number of oxygen vacancies associated with randomly distributed pentacoordinated Fe^{3+} ions [15]; the vacancies are mainly disordered and σ_{ion} increases accordingly. With iron substitution levels greater than 40 mol%, σ_{ion} is strongly reduced by the increasing number of ordered anion vacancies around the stable tetracoordinated Fe^{3+} ions which eventually give rise to fully ordered phases [15]. It should be noticed that there is no apparent effect of the lattice ordering on the electronic conductivity, which increases with x [11, 12].

The present simplified description suffices to understand the effect of composition, but microstructure and the surface exchange also have an important role especially for the composition with better performance ($x = 0.20$). $CaTi_{0.8}Fe_{0.2}O_{3-\delta}$ is actually a partially ordered phase with a rather complex structure in which the iron cations may easily assume different valences or coordination (either hexa- or penta-coordinated Fe^{4+} and hexa-, penta- and tetracoordinated Fe^{3+}) thus having a significant influence on σ_{ion}. The slight bend observed in the jo_2 vs. $1/T$ dependence (Fig. 7) for this composition was explained as the result of a decrease in σ_{ion} due to microstructural changes associated to the existence of structural microdomains and oxygen vacancy ordering [30]. In fact, ceramics with the same nominal composition ($x = 0.20$) but different microstructure showed differences in measured jo_2 values as large as 50%, under relatively small oxygen chemical potential gradients. Considerably larger differences may therefore occur when much larger gradients are used. This more than likely possibility is supported by the significant differences found in the values of conductivity measured in H_2/N_2 and CO/CO_2 gas mixtures [31]. However, to the best of our knowledge results of

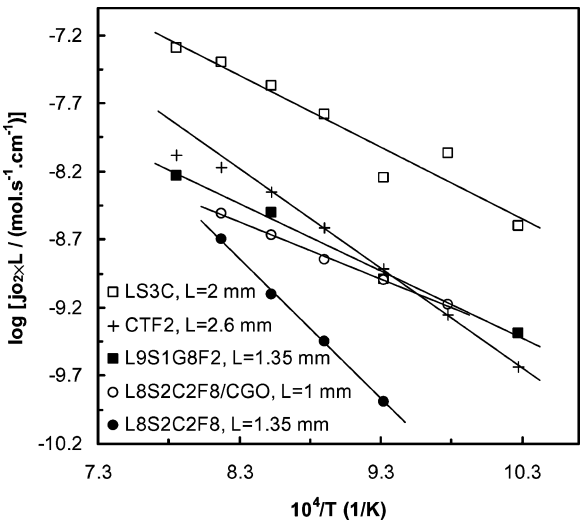

Fig. 9. Comparison of the oxygen permeation of $CaTi_{0.8}Fe_{0.2}O_{3-\delta}$ with other materials at constant Po_2 gradient (log $(P_2/P_1) \approx 1$ and $P_1 = 21$ kPa). All data were obtained using the same experimental technique. LS3C – $La_{0.7}Sr_{0.3}CoO_{3-\delta}$ [33], CaTF2 - $CaTi_{0.8}Fe_{0.2}O_{3-\delta}$ [this work], L9S1G8F2 – $La_{0.9}Sr_{0.1}Ga_{0.8}Fe_{0.2}O_{3-\delta}$ [34], L8S2C2F8/CGO – $La_{0.8}Sr_{0.2}Co_{0.2}Fe_{0.8}O_{3-\delta}/Ce_{0.8}Gd_{0.2}O_{2-\delta}$ composite [35], L8S2C2F8 - $La_{0.8}Sr_{0.2}Co_{0.2}Fe_{0.8}O_{3-\delta}$ [35].

oxygen permeation of $CaTi_{1-x}Fe_xO_{3-\delta}$ under large Po_2 gradients were not yet reported.

Figure 9 compares the oxygen permeability of several materials. The results were obtained using the same experimental technique under oxidising conditions and a small Po_2 gradient established between 21 kPa and ≈ 0.21 kPa. It may be seen that the performance of $CaTi_{0.8}Fe_{0.2}O_{3-\delta}$ is comparable to that of some of the alternative materials based in Co- and Sr-containing compositions, yet worse than that of $La_{1-x}Sr_xCoO_{3-\delta}$ ($x = 0.30$). The thermal expansion of the latter material is, however, considerably higher (about $21 \times 10^{-6}\ K^{-1}$) and it quickly decomposes at high temperature when the Po_2 is lower than approximately 1 Pa [32].

4. Conclusions

The direct comparison of the overall performances of $CaTi_{0.80}Fe_{0.20}O_{3-\delta}$ and of other mixed conducting materials for oxygen separation membranes demonstrates the viability of $CaTi_{0.80}Fe_{0.20}O_{3-\delta}$ as an oxygen electrochemical permeation membrane, since it combines oxygen permeation with good chemical and thermo-mechanical stability. Contrary to many other mixed conducting materials, the thermal expansion of $CaTi_{1-x}Fe_xO_{3-\delta}$ ceramics shows a linear behaviour over a relatively large temperature range, from room temperature to 1000°C. The estimated linear thermal expansion coefficient is close to $13 \times 10^{-6}\ K^{-1}$ for all compositions and shows a good agreement with the values estimated from the variation of the lattice volume with temperature. No evidence for formation of carbonated products of the reaction of $CaTi_{1-x}Fe_xO_{3-\delta}$ with CO_2 at room temperature could be found in IR absorption spectra.

While the stability and thermal expansion are apparently not influenced by composition, the oxygen permeation is, and quite significantly. Differences of two orders of magnitude were found in the oxygen permeability fluxes measured at temperatures ranging from 750 to 1000°C and under small Po_2 gradients. The best performance was obtained for the $x = 0.20$ composition, showing typical values for the molecular oxygen flux of 2.0×10^{-8} mol s^{-1} cm^{-2} at 900°C under a Po_2 gradient established between 21×10^3 and 686 Pa. The values for $x = 0.05$ and 0.60 were more than one order of magnitude lower, under the same conditions. The sharp maximum for $x = 0.20$ is consistent with changes in the ionic conductivity due to structural differences related to a balance in the concentration of ordered and disordered oxygen vacancies. The results also suggest that the oxygen surface exchange is the major limiting factor to permeability if thin membranes are used. The characteristics of the materials in the $CaTi_{1-x}Fe_xO_{3-\delta}$ compositional range studied in this work seem particularly suitable for the development of multilayered membranes since one may tailor the electrical properties without compromising the chemical and thermo-mechanical compatibility between layers.

Acknowledgements

Financial support by the FCT, Portugal (PRAXIS and POCTI programs), NATO Science for Peace program (project 978002), INTAS (project 00276), and the Belarus Ministry of Education made this work possible. A special thanks to Juan Rubio from the ICV (Madrid) for providing the $CaCO_3$ IR spectra.

References

1. H. Iwahara, T. Esaka, and T. Mangahara, *J. Appl. Electrochem*, **18**, 173 (1988).
2. U. Balachandran, T.J. Dusek, S.M. Sweeney, R.B. Poeppel, R.L. Mieville, P.S. Maiya, M.S. Kleefisch, S. Pei, T.P. Kobylinski, C.A. Udovich, and A.C. Bose, *Am. Ceram. Soc. Bull.*, **74**(1), 71 (1995).
3. H.J.M. Bouwmeester, H. Kruidhof, and A.J. Burggraf, *Solid State Ionics*, **72**, 185 (1994).
4. M.F. Carolan, P.N. Dyer, J.M. LaBar, and R.M. Thorogood, US Patent 5,261,932 (1993).
5. M.F. Carolan, P.N. Dyer, S.A. Motika, and P.B. Alba, US Patent 5,712,220 (1998).
6. Y. Teraoka, H.M.Y. Zhang, K. Okamoto, and N. Yamazoe, *Mat. Res. Bull.*, **23**, 51 (1988).
7. D. Sujita, T. Norby, P.A. Osborg, and P. Kosftad, *Electrochem., Soc. Proc.*, **93–4**, 552 (1993).
8. S. Marion, A.I. Becerro, and T. Norby, *Ionics*, **5**, 385 (1999).
9. L.A. Dunyushkina, A.K. Demin, and B.V. Zhuralev, *Solid State Ionics*, **116**, 85 (1999).
10. S. Marion, A.I. Becerro, and T. Norby, *Phase Transitions*, **69**, 157 (1999).
11. F.M. Figueiredo, J.C. Waerenborgh, V.V. Kharton, H. Näffe, and J.R. Frade, *Solid State Ionics*, **156**, 371 (2003).
12. C. McCammon, A.I. Becerro, F. Langenhorst, R. Angel, S. Marion, and F. Seifert, *J. Phys.: Condens. Matter*, **12**, 2969 (2000).
13. J.-C. Grenier, G. Schiffmacher, P. Caro, M. Pouchard, and P. Hagenmuller, *J. Solid State Chem.*, **20**, 365 (1977).
14. J.-C. Grenier, M. Pouchard, P. Hagenmuller, G. Schiffmacher, and P. Caro, *J. Physique Colloque*, **C7 38**, C7-84 (1977).

15. J.C. Waerenborgh, F.M. Figueiredo, J.R. Jurado, and J.R. Frade, *J. Phys.: Condens. Matter*., **13**, 8171 (2001).
16. J.-C. Grenier, M. Pouchard, P. Hagenmuller, M.J.R. Enche, M. Vallet, J.M.G. Calbet, and M.A. Alario-Franco, *Revue Chimie Minérale*, **20**, 726 (1983).
17. T. Esaka, T. Fujii, K. Suwa, and H. Iwahara, *Solid State Ionics*, **40/41**, 544 (1990).
18. V.V. Kharton, F.M. Figueiredo, A.V. Kovalevsky, A.P. Viskup, E.N. Naumovich, J.R. Jurado, and J.R. Frade, *Defect and Diffusion Forum*, **186/187**, 119 (2000).
19. E. Chinarro, J.R. Jurado, F.M. Figueiredo, and J.R. Frade, *Solid State Ionics*, **160**, 161 (2003).
20. F.M. Figueiredo, J.R. Frade, and F.M.B. Marques, *Solid State Ionics*, **110**, 45 (1998).
21. F.M. Figueiredo, F.M.B. Marques, and J.R. Frade, *Solid State Ionics*, **138**, 173 (2001).
22. S.A.T. Redfern, *J. Phys.: Condens. Matter*, **8**, 8267 (1996).
23. J. Canales-Vázquez, F.M. Figueiredo, J.C. Waerenborgh, W. Zhou, J.R. Frade, and John T.S. Irvine, *J. Solid State Chem.*, **177**, 3105 (2004).
24. J.R. Jurado, F.M. Figueiredo, B. Gharbage, and J.R.Frade, *Solid State Ionics*, **118**, 89 (1999).
25. V.V. Kharton, A.A. Yaremchenko, A.P. Viskup, M.V. Patrakeev, I.A. Leonidov, V.L. Kozhevnikov, F.M. Figueiredo, A.L. Shaulo, E.N. Naumovich, and F.M.B. Marques, *J. Electrochem. Soc.*, **149**(4), E125 (2002).
26. H. Hayashi, M. Suzuki, and H. Inaba, *Solid State Ionics*, **128**, 131 (2000).
27. *Lange's Handbook of Chemistry*, 12th ed., edited by J.A. Dean (McGraw-Hill, New York, 1978.) chap. 9.
28. V.V. Kharton, A.P. Viskup, A.V. Kovalevsky, F.M. Figueiredo, J.R. Jurado, A.A. Yaremchenko, E.N. Naumovich, and J.R. Frade, *J. Materials Chemistry*, **10**, 1161 (2000).
29. C.H. Perry, B.N. Khanna, and G. Rupprecht, *Physical Review*, **133**, A408 (1964).
30. F.M. Figueiredo, V.V. Kharton, J.C. Waerenborgh, A.P. Viskup, E.N. Naumovich, and J.R. Frade, "Influence of Microstructure on the Electrical Properties of Iron-Substituted Calcium Titanate Ceramics," *J. Am. Ceram. Soc.*, in press.
31. A. Selçuk and B.C.H. Steele, *Fourth Euro Ceramics*, edited G. Gusmano and E. Traversa (Editoriale Faenza Editrice S.p.A., 1995, 413) Vol. 5.
32. T. Nakamura, G. Petzow, and L.J. Gaukler, *Mat. Res. Bull.*, **14**, 649 (1979).
33. F.M. Figueiredo, F.M.B. Marques, and J.R.Frade, *Solid State Ionics*, **111**, 273 (1998).
34. B. Gharbage, F.M. Figueiredo, R.T. Baker, and F.M.B. Marques, *Electrochimica Acta*, **45**(13), 2095 (2000).
35. V.V. Kharton, A.V. Kovalevsky, A.P. Viskup, A.L. Shaulo, F.M. Figueiredo, E.N. Naumovich, and F.M.B. Marques, *Solid State Ionics*, **160**, 247 (2003).
36. F.S. Galasson, *Structure, Properties and Preparation of Perovskite Compounds* (Pergamon, Oxford, 1969), p. 163.